SHANNON, R. D. (1976). *Acta Cryst.* A**32**, 751-767.
TANAKA, M., SAITO, R. & WATANABE, D. (1980). *Acta Cryst.* A**36**, 350-352.
TSUNEKAWA, S., SUEZAWA, M. & TAKEI, H. (1977). *Phys. Status Solidi A*, **40**, 437-446.
TSUNEKAWA, S. & TAKEI, H. (1978). *Phys. Status Solidi A*, **50**, 695-702.
WATANABE, N., ASANO, H., IWASA, H., SATOH, S., MURATA, H., KARAHASHI, K., TOMIYOSHI, S., IZUMI, F. & INOUE, K. (1987). *Jpn. J. Appl. Phys.* **26**, 1164-1169.

Acta Cryst. (1993). A**49**, 600–605

Phase Determination of X-ray Reflections in a Quasicrystal

BY H. LEE AND R. COLELLA

Purdue University, Physics Department, West Lafayette, Indiana 47907, *USA*

AND L. D. CHAPMAN

Brookhaven National Laboratory, National Synchrotron Light Source, Upton, New York 11973, *USA*

(*Received* 10 *June* 1992; *accepted* 15 *December* 1992)

Abstract

Multiple Bragg diffraction effects have been observed in an Al-Cu-Fe quasicrystal. The experimental data are analyzed by means of a multibeam perturbation theory. Good fits are obtained between experimental and calculated profiles. The feasibility for phase determination of structure factors is demonstrated. It is found that there is no inversion symmetry in Al–Cu–Fe.

1. Introduction

It has been shown recently that multiple Bragg scattering can be used for phase determination of X-ray structure factors (Shen & Colella, 1987). The general idea is to monitor the intensity of a weak reflection as the crystal is rotated around the scattering vector. When a strong reflection is excited simultaneously, the diffracted intensity exhibits a peak as a function of ψ, the azimuthal angle of rotation, with asymmetric side bands. It has been pointed out (Chapman, Yoder & Colella, 1981) that phase information can be obtained from the asymmetric side bands using n-beam dynamical theory, even when dealing with mosaic crystals of general shape (Shen & Colella, 1987).

A general review of multibeam literature was published a few years ago (Chang, 1987) and recently phase effects have been observed in protein crystals (Hümmer, Schwegle & Weckert, 1991; Chang, King, Huang & Gao, 1991).

In this paper we report the observation of multiple-diffraction (Renninger) effects in a quasicrystal. Since a quasicrystal does not possess long-range periodicity in the usual sense, it is not clear that all diffraction features present in ordinary crystals should be visible in quasicrystals. However, we know that strong and sharp Bragg diffraction spots are produced by quasicrystals. We also know how to predict the positions of nodes in reciprocal space.* A necessary condition for the existence of the Renninger effect is that the difference between the Miller indices of two Bragg reflections must also correspond to a Bragg reflection. Since the xyz coordinates of every node in reciprocal space are expressed by means of a linear combination of six Miller indices, the necessary condition mentioned above is certainly satisfied in a quasicrystal.

2. Experimental

Since multiple-beam effects are more visible for weak reflections, we decided to concentrate on the reflection $2\bar{4}044\bar{2} = \mathbf{P}$, which was chosen on the basis of a precession photograph taken perpendicularly to the fivefold axis. Bragg nodes in reciprocal space are referred to three orthogonal x, y, z axes, coinciding with the three twofold axes of the icosahedron. The x, y, z coordinates of a reciprocal-lattice vector, whose Miller indices are n_1, n_2, n_3, n_4, n_5, n_6, are given in this paper by

$$\mathbf{G}_\parallel = K \sum_{i=1}^{6} n_i \mathbf{e}_\parallel^i, \qquad (1)$$

where

$$K = 1/[2\pi a(1+\tau^2)^{1/2}], \quad \tau = \frac{(1+5^{1/2})}{2}, \qquad (2)$$

* In this work we label Bragg spots with the sixfold Miller indices notation due to Elser (1986).

ISSN 0108-7673

a is the quasilattice constant and the xyz components of the $\mathbf{e}_\parallel^i$ basis vectors are:

$$\mathbf{e}_\parallel^1=\begin{pmatrix}0\\1\\\tau\end{pmatrix},\quad \mathbf{e}_\parallel^2=\begin{pmatrix}\tau\\0\\1\end{pmatrix};\quad \mathbf{e}_\parallel^3=\begin{pmatrix}1\\\tau\\0\end{pmatrix};$$
$$\mathbf{e}_\parallel^4=\begin{pmatrix}-1\\\tau\\0\end{pmatrix};\quad \mathbf{e}_\parallel^5=\begin{pmatrix}-\tau\\0\\1\end{pmatrix};\quad \mathbf{e}_\parallel^6=\begin{pmatrix}0\\-1\\\tau\end{pmatrix}. \tag{3}$$

A small fragment ($0.1\times0.07\times0.07$ mm) was chipped off a large boule of $Al_{63.7}Cu_{23.6}Fe_{12.7}$ quasicrystal.* It was found by precession photography that the only way to get a single and clean diffraction pattern was to use very small fragments. Precession photographs were also taken along the twofold and threefold axes. From these photographs, a value for the quasilattice constant, $a=2.8425$ Å, was deduced. The crystal was glued with Duco cement to the tip of a thin (0.1 mm diameter) glass fiber and mounted on a standard Eulerian goniometer. The crystal was oriented so that the **P** scattering vector was parallel to the spindle axis and the fivefold axis was perpendicular.

To calculate the azimuthal positions at which Renninger peaks† might be observable, we used the set of Bragg reflections observed by powder diffraction.‡

The experiments were performed at beam line X-18A of the National Synchrotron Light Source (NSLS) at Brookhaven National Laboratory. The wavelength of the X-ray beam was $\lambda=1.545$ Å.

It was found initially that, despite our extensive and careful searches, only a very small fraction of the predicted Renninger peaks were visible. Since a condition for the observability of Renninger peaks for a weak **P** reflection is that the simultaneous reflection, **H**, and the coupling reflection, **P–H**, both be strong, we felt the need for a criterion to classify strong and weak reflections. For this purpose, we used a formalism developed by Elser (1986) for a monoatomic quasicrystal. We found that Elser's formula, for the spots present on our precession photographs, was always in qualitative agreement with experiment.

When the intensities of the simultaneous and coupling reflections were evaluated with Elser's formula, it became immediately clear why so few Renninger peaks are visible. The only peaks we were able to observe corresponded to simultaneous and coupling reflections that were both strong. Figs. 1, 2 and 3 are examples of our observations. Each point in these plots represents the maximum of an ω scan, to make sure that the crystal is always perfectly oriented for all values of the azimuthal angle ψ. Since the crystal is a mosaic, each point is proportional to the integrated intensity, which is the quantity to be used for comparison with theory.

In all these profiles the asymmetry effect (Chapman, Yoder & Colella, 1981) is clearly visible, which indicates that some interference action is taking place, with opposite signs on the two sides of the Renninger peak. We can then conclude, at this point, that the degree of long-range ordering present in a quasicrystal is not only sufficient to produce Bragg reflections, it can also produce visible interference effects between different Bragg reflections excited at the same time. It is important to realize that the two peaks of Figs. 1 and 2 are symmetry related and should be mirror images of each other. The difference in the rocking widths is caused by the mosaic structure of the crystal and the difference in the horizontal resolutions. The two profiles were recorded in two different experiments. The beam of X-18A is horizontally focused with a mirror. The nominal convergence angle of the beam leaving the mirror is 7 mrad. However, the beam is not focused to a point and a small crystal will subtend a smaller fraction of the nominal 7 mrad. The actual fraction of beam subtended depends critically on the position of the crystal in the focal spot and is not easy to control. We believe that the difference in shape of the profiles in Figs. 1 and 2 originates for the most part from the different conditions of horizontal resolution present in the two cases. This conjecture is confirmed by our theoretical fitting procedure, as will be shown later.

3. Analysis

Once the existence of the Renninger effect with its phase-related asymmetry is definitely established for a quasicrystal, the problem to be tackled is how to analyze these results. The theory normally used for regular crystals (Colella, 1974; Shen, 1986) is based on the assumption of a triply periodic medium, which is not the case for a quasicrystal. However, Bragg reflections do exist in a quasicrystal. The theory of n-beam diffraction in regular crystals is essentially based on the ability to express the electromagnetic field in the medium in terms of Ewald waves (Colella, 1974):

$$\mathbf{D}(\mathbf{r})=\sum_{i=1}^{4N}\Psi^i\sum_H\mathbf{D}_H^i\exp\left(-2\pi i\boldsymbol{\beta}_H^i\cdot\mathbf{r}\right). \tag{4}$$

Equation (4) also applies to a quasicrystal, for the existing Bragg reflections, and therefore the treatments given by Colella (1974) and Shen (1986) are applicable.

* The material was prepared by Dr P. Bancel at IBM.

† A Renninger peak is a peak observed in a plot in which the intensity of a given Bragg reflection **P** is plotted against ψ, the azimuthal rotation angle around the scattering vector **P**.

‡ Courtesy of Dr P. Bancel.

The situation is somewhat similar to that of an incommensurate modulated structure. For example, it has been shown (Colella, 1982) that the n-beam treatment given by Colella (1974) can explain quantitatively the side bands observed in rocking curves of perfect crystals (InSb) in which strong beams of monochromatic phonons were excited using the acoustoelectric effect.

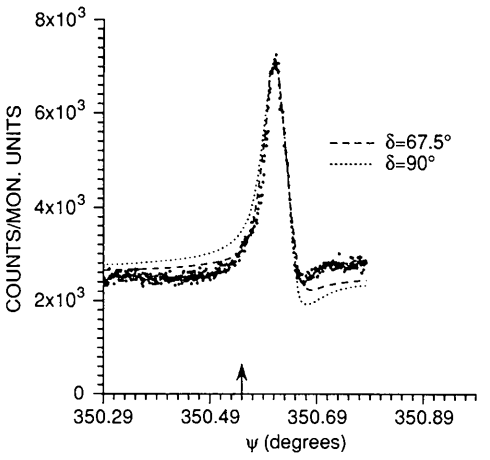

Fig. 1. Intensity of the weak $2\bar{4}044\bar{2}=\mathbf{P}$ reflection as a function of the azimuthal angle ψ, when the crystal is rotated around the scattering vector. The angle ψ is zero when the $00\bar{1}000$ axis is in the scattering plane, mostly antiparallel to the incident beam. The ψ angle is calculated from the spectrometer angles χ, φ and θ. The arrow indicates the position where the peak was expected. Two simultaneous reflections are excited at the same angle $0\bar{4}042\bar{2}=\mathbf{H}_1$ and $400242=\mathbf{H}_2$. The dashed and dotted lines are theoretical fits with different values for the phase of the $\mathbf{H}_1$ reflection with respect to $\mathbf{P}$. The counting time per point was approximately 2 s. X-ray energy: 8.02 keV.

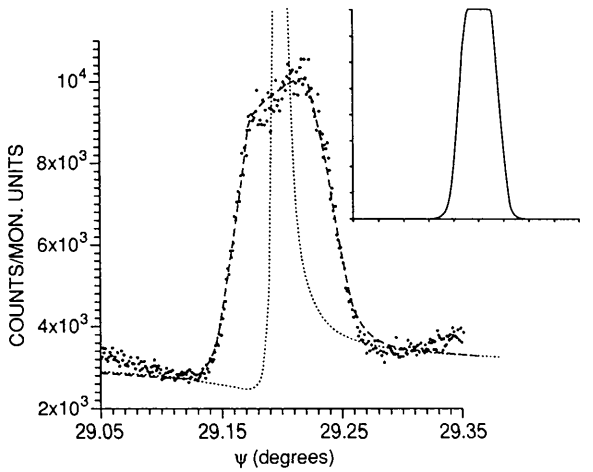

Fig. 2. The same as Fig. 1 except that now $\mathbf{H}'_1=2\bar{2}0440$ and $\mathbf{H}'_2=\bar{2}40204$. The value ψ_0 at which the peak is expected is $\psi_0=9.50°$. In this run, the zero on the ψ scale was set at 19.70. This peak is the mirror image of that shown in Fig. 1. The difference in peak width is due to a different effect of the mosaic spread and to a difference in horizontal beam divergence (normal to the scattering plane). The dashed line is a fit with the phase difference between $\mathbf{H}'_1$ and $\mathbf{P}$ equal to 67.5°, the same value that gives the best fit in Fig. 1. The dotted line is the unconvoluted profile. The inset shows the smearing function used for this fit (see text).

In the case of a quasicrystal, we can say that, along certain directions, spatial coherence between 'lattice planes' is sufficiently preserved to allow strong Bragg reflections to be excited. Presumably, dynamical effects will also be present. The situation is reminiscent of that of thermal motion in a perfect crystal, which does not prevent, for instance, the onset of anomalous transmission. In fact, it has recently been proposed (Berenson & Birman, 1986) that anomalous transmission may be present in a quasicrystal.

Having convinced ourselves of the legitimacy of the use of n-beam dynamical theory for quasicrystals, we have analyzed the experimental profiles of Figs. 1, 2 and 3 with a view to obtaining phase information. As a zero-order approximation, structure factors have been calculated with a formula given by Elser (1986) for a monoatomic quasicrystal, with average values for the scattering factors. In calculating structure factors, there is a problem in specifying the value of an arbitrary scale factor, related to the volume over which the structure factor is evaluated (Elser, 1991). As a starting point, we have taken the scaling factor to be 1 and have obtained good-quality fits. Values differing from 1 by τ or $1/\tau$ would have made our fits more difficult and of inferior quality. In our definitions, all phases, for all structure factors, are initially set equal to 0.

Table 1 shows all the structure factors used in the present work. The central column shows the geometrical part $F^0_{\mathbf{H}}$ of the structure factor given by

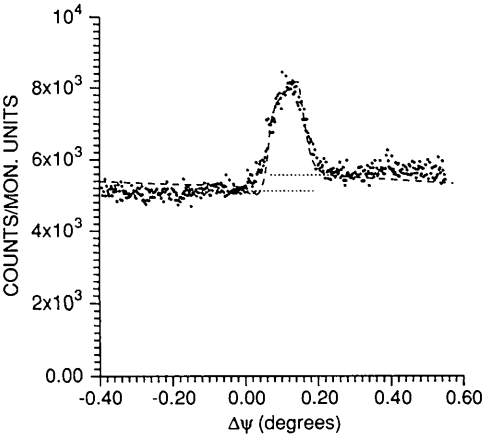

Fig. 3. The same as Fig. 1, except that only one simultaneous reflection is excited, $\bar{2}04\bar{4}02$. $\Delta\psi$ is the difference $\psi-\psi_0$, where ψ_0 is the angle at which the peak is expected ($\psi_0=-34.71°$). The asymmetry effect is evident in the two different background levels, on the two sides of the peak. This peak can be fitted with a theoretical profile (dashed line) with zero phase difference between structure factors.

Table 1. *Values of structure factors used in the present work*

The first column lists all reflections involved (main, simultaneous and coupling reflections). The second column gives the sixfold Miller indices (in the notation of Elser, 1986). The third column gives the structure factors calculated from the theory given by Elser (1986), valid for a monoatomic crystal. The numbers listed in the fourth column are obtained by multiplication of the numbers of the third column by a scattering factor equal to a weighted average between Al, Cu and Fe. No attempt is made to include thermal factors.

Reflection	Miller indices	$F_{\mathbf{H}}^0$	F_H (electron units)
P	$2\bar{4}044\bar{2}$	1.119	12.87
$\mathbf{H}_1$	$0\bar{4}042\bar{2}$	4.953	61.35
$\mathbf{H}_2$	400242	4.953	61.35
$\mathbf{P}-\mathbf{H}_1$	200020	1.156	18.74
$\mathbf{P}-\mathbf{H}_2$	$2\bar{4}020\bar{4}$	4.953	61.35
$\mathbf{H}_1'$	$2\bar{2}0440$	4.953	61.35
$\mathbf{H}_2'$	$2\bar{4}020\bar{4}$	4.953	61.35
$\mathbf{P}-\mathbf{H}_1'$	$0\bar{2}000\bar{2}$	1.156	18.74
$\mathbf{P}-\mathbf{H}_2'$	400242	4.953	61.35
$\mathbf{H}_3$	$\bar{2}0\bar{4}\bar{4}02$	4.953	61.35
$\mathbf{P}-\mathbf{H}_3$	$4\bar{4}484\bar{4}$	0.979	8.083

Elser's formula and the right column shows the structure factor $F_{\mathbf{H}}$ in electron units for the assumption of a monoatomic crystal with a scattering factor equal to a weighted average between those of Al, Cu and Fe.

What the n-beam experiment provides is a value for the triplet invariant (Shen & Colella, 1987)

$$\delta = \varphi_{\mathbf{H}} + \varphi_{\mathbf{P}-\mathbf{H}} - \varphi_{\mathbf{P}}, \tag{5}$$

in which **P** is the main reflection, **H** is the simultaneous reflection and $\mathbf{P}-\mathbf{H}$ is the coupling reflection. In our case, the assumed value of δ is obviously zero, which is equivalent to the assumption that the crystal is centrosymmetric.

The smooth profiles of Figs. 1 to 3 have been calculated with use of the perturbation theory developed by Shen (1986), which has been proved (Tischler, Shen & Colella, 1985) to be very accurate on the tails of the Renninger peaks but obviously fails at the exact multibeam-excitation point on the ψ scale. The peak intensity becomes infinite at this point.

The crystal is assumed to be perfect (zero mosaic spread) and the beam perfectly parallel (zero divergence). Since there is no way to calculate the experimental maximum value of a Renninger peak,* we decided to truncate the calculated profiles to a value that provides a good fit with experiment. This truncation value is the only arbitrary adjustable parameter of our fits. A smearing function was then convoluted with the theoretical profiles. The profiles of Fig. 1 have been obtained with a Gaussian smearing function, whose FWHM was 2.7′, in qualitative agreement with the peak width observed in ω scans. For the peak of Fig. 2, we used a step function in which the two vertical sides were replaced with the two halves of the Gaussian used for Fig. 1 (see inset). This replacement was made because of the angular convergence of the incident beam coming from the mirror, as explained earlier. Every attempt to fit the profile of Fig. 2 with a wide Gaussian failed. Since the smearing function has a flat top, it is clear that the inclined top of the profile of Fig. 2 is a direct indication of the strong asymmetry present in the unconvoluted profile (dotted line). The Renninger peaks of Figs. 1 and 2 are four-beam cases. ($\mathbf{H}_1$, $\mathbf{H}_2$, $\mathbf{H}_1'$, $\mathbf{H}_2'$, are the simultaneous reflections; see Table 1.) It has been shown by perturbation theory (Shen, 1986) that, in this case, two triplet invariants should be considered: δ_1, due to **P** interacting with $\mathbf{H}_1$, and δ_2, due to **P** interacting with $\mathbf{H}_2$. In fact, equation (23a) of Shen (1986), adapted to our four-beam case, reads

$$I_\perp = 1 + 2\gamma_{\mathbf{PH}_1}(\cos\delta_{\mathbf{PH}_1})(K_{\mathbf{H}}^2 - H_{1\sigma}^2)/(k_0^2 - k_{\mathbf{H}_1}^2) + 2\gamma_{\mathbf{PH}_2}(\cos\delta_{\mathbf{PH}_2})(K_{\mathbf{H}_2}^2 - H_{2\sigma}^2)/(k_0^2 - k_{\mathbf{H}_2}^2), \tag{6}$$

where $I_\perp$ is the integrated intensity (over θ, the angle of incidence on the lattice planes of the **P** reflection; only the perpendicular component needs to be considered in a synchrotron experiment) and the other symbols are defined by Shen (1986) as

$$H_{1\sigma} = \mathbf{H}_1 \cdot \boldsymbol{\sigma}; \quad H_{2\sigma} = \mathbf{H}_2 \cdot \boldsymbol{\sigma}; \quad k_0 = 1/\lambda;$$

$\boldsymbol{\sigma}$ = unit vector, normal to the scattering plane defined by $\mathbf{k}_0$ and **P**;

$$\gamma_{\mathbf{PH}_1} = \Gamma|(F_{\mathbf{P}-\mathbf{H}_1}F_{\mathbf{H}_1})/F_{\mathbf{P}}|;$$

$$\gamma_{\mathbf{PH}_2} = \Gamma|(F_{\mathbf{P}-\mathbf{H}_2}F_{\mathbf{H}_2})/F_{\mathbf{P}}|;$$

$$\Gamma = r_e\lambda^2/\pi V_C;$$

r_e = classical radius of electron;

V_C = volume of the unit cell;

$$\delta_{\mathbf{PH}_1} = \varphi_{\mathbf{H}_1} + \varphi_{\mathbf{P}-\mathbf{H}_1} - \varphi_{\mathbf{P}};$$

$$\delta_{\mathbf{PH}_2} = \varphi_{\mathbf{H}_2} + \varphi_{\mathbf{P}-\mathbf{H}_2} - \varphi_{\mathbf{P}}.$$

The second term present in Shen's equation (23a) has been dropped because it is usually negligible in comparison with the third term, as a result of the denominator being squared.

The fittings of Figs. 1, 2 and 3 are with respect to δ_1. Use of δ_2 gave unreasonable fits.

It should be realized that the occurrence of two simultaneous reflections for a given azimuth (giving rise to a four-beam case) is not accidental. It is related to the symmetry properties of the **P** point in reciprocal space and it does not depend on the particular value

* The exact theoretical treatment given by Colella (1974) could be used, but the peak value calculated in this way would be valid for a perfect crystal, not for a crystal with mosaic spread. The difference in the diffracted intensities by a perfect and a mosaic crystal vanishes on the side bands, because the scattering is weak there, but cannot be neglected at the maximum of a Renninger peak, where the scattering is strong.

of λ chosen (in our experiment, $\lambda = 1.545$ Å). If we consider the case in which $\mathbf{H}_1$ and $\mathbf{H}_2$ are the simultaneous reflections (see Table 1), it turns out that, as the azimuthal angle ψ is increased through the exact value for multibeam excitation (see arrow in Fig. 1), H_1 enters the Ewald sphere (out-in) and H_2 exits the sphere (in-out). This behavior is connected with the sign of the multibeam perturbation over the two-beam value, in relation to the sign of the denominators in (6). It may be added at this point that the small differences between calculated and observed azimuthal angles at which the Renninger peaks are detected are due to experimental errors.

If the profiles of Figs. 1 and 2 are calculated with the two triplet invariants δ_1 and δ_2 equal to zero, the asymmetry is reversed. The best agreement, for both Fig. 1 and Fig. 2, is obtained with $\delta_1 = 67.5 \pm 20$ and $\delta_2 = 0°$. In Fig. 1, we show that a profile corresponding to $\delta_1 = 90°$ does not fit well. In a standard three-beam case, a triplet invariant of 90° would produce a profile with no asymmetry, because the perturbation term in (6) would be multiplied by $\cos 90° = 0$.

In our case, however, we have four beams and a noticeable asymmetry is present with $\delta_1 = 90$, $\delta_2 = 0°$, due to the action of the third term in (6). $\delta_1 = 45°$ would also give a bad fit. Since, for a centrosymmetric structure, every triplet invariant δ can only have two values, 0 or π, we can conclude that the Al-Cu-Fe quasicrystal is not centrosymmetric. We wish to emphasize that this conclusion is independent of the particular form used to express the structure factors. In fact, in principle, we can use the following definition for a structure factor:

$$F_{\mathbf{H}}^{qc} = \sum_{i=1}^{N} f_i \exp\left[2\pi i(\mathbf{H} \cdot \mathbf{r}_i)\right], \qquad (7)$$

where f_i are the atomic scattering factors, $\mathbf{r}_i$ are the atomic positions referred to an arbitrary origin and N is the *total number of atoms in the crystal.* The quantity of interest is $F_{\mathbf{H}}^{qc}/V_{qc}$, where V_{qc} is the volume of the quasicrystal. In a regular crystal the quantity of interest is $F_{\mathbf{H}}/V_c$, where the sum is evaluated in a unit cell and V_C is the volume of such a unit cell. In a quasicrystal there is no universal consensus on how $F_{\mathbf{H}}^{qc}/V_{qc}$ should be written but, depending on the model used, a suitable expression for $F_{\mathbf{H}}^{qc}/V_{qc}$ can be determined and used in the formulae for calculating intensities. There is no doubt that, whatever model is used and whatever expression is adopted for $F_{\mathbf{H}}^{qc}/V_{qc}$, the resultant value must be equal to that given by (7). The notion of 'phase of a structure factor' in a quasicrystal is therefore not model dependent but it can be established on an absolute basis with use of (7).

Another example is given in Fig. 3. The same smearing function used for Fig. 2 has been applied here. Again, the asymmetry effect is clearly visible in the different background levels on the sides of the peak. In this case, δ has been set equal to zero.

4. Discussion and concluding remarks

Since a quasicrystal is not a periodic structure, the notion of centrosymmetry (or lack of it) can only be established in the whole crystal. On the other hand, owing to the lack of long-range periodicity, no two pieces of the same quasicrystalline material are identical. If we cut a big quasicrystal into, say, ten pieces, their diffraction patterns are not expected to be absolutely identical (neglecting for a moment size effects), although we doubt that any discernible difference will be visible. Therefore, the presence (or absence) of centrosymmetry can only be established *on the average.* It may be useful to compare this with a regular periodic crystal subject to thermal motion. We can say that the ten pieces resulting from cutting a large quasicrystal are the analog of an 'ensemble' of systems, in the sense of statistical mechanics. The 'average structure' is the analog of an ensemble average. In other words, the ten small quasicrystals constitute a set that is related to the average structure mentioned above in generally the same way as several instantaneous snapshots of a regular periodic crystal subject to thermal motion are related to its ideal periodic static structure.

Our conclusion, from the analysis of Figs. 1 and 2, is then that there is no point in the crystal that can be taken as a center of symmetry.

The question of the presence or absence of centrosymmetry is of crucial importance for the determination of atomic locations. So far, most of the work in this area has been done with use of a method based on contrast-variation effects in neutron diffraction (Janot, Pannetier, De Boissieu & Dubois, 1987). It was found by Janot *et al.* (1987) that the Al-Si-Mn quasicrystal is centrosymmetric. This result was arrived at by comparison of the intensities of selected Bragg reflections in powder samples in which manganese (a negative neutron scatterer) was replaced with Fe or FeCr (positive neutron scatterers). The same result (centrosymmetry) was found in several other icosahedral structures, other than Al-Cu-Fe, investigated by the same method. Since the presence or absence of centrosymmetry is a minor perturbation on the intensities of most Bragg reflections, it is very difficult to draw firm conclusions from powder diffraction data.

On the other hand, detailed structural data on single-crystal Al-Cu-Fe have recently been obtained with use of neutron diffraction (Cornier-Quiquandon, Quivy, Lefèbvre, Elkaim, Heger, Katz & Gratias, 1991). The structural analysis was based on the Patterson method and the assumption was made that the structure is centrosymmetric with icosahedral point

group $m\bar{3}\bar{5}$, as opposed to 235 (noncentrosymmetric). The reasons for this choice of point group are explained by the authors in terms of transmission electron microscopy (TEM) analysis. No inversion domains could be found in TEM images of Al–Cu–Fe samples [Rzepski, Quivy, Calvayrac, Cornier-Quiquandon & Gratias (1989), § 3; Cornier-Quiquandon, Quivy, Lefèbvre, Elkaim, Heger, Katz & Gratias (1991), footnote 36]. In other words, no convincing evidence of lack of centrosymmetry was found and centrosymmetry could not be ruled out altogether.

In conclusion, we have demonstrated the feasibility of phasing structure factors in a quasicrystal with use of multiple Bragg scattering. The phase values for the triplet invariants obtained by this method are model independent and can be used to assess different structural models.

Special thanks are due to P. Bancel who provided the material used in this work and offered invaluable technical assistance in understanding the physics of quasicrystals. The authors are indebted to V. Elser for several extensive discussions. The generous help of S. Ehrlich and X. Yang of NSLS and J. Arthur of SSRL in recording the synchrotron data is deeply appreciated. Thanks are also due to D. Gratias for many illuminating discussions on basic issues of quasicrystallography.

This work was supported by NSF Grant DMR-8715503 and by a DOE Grant DE-FG02-85ER45183, which supports the operations of beamline X-18A at NSLS.

References

BERENSON, R. & BIRMAN, J. L. (1986). *Phys. Rev. B*, **34**, 8926–8928.
CHANG, S. L. (1987). *Crystallogr. Rev.* **1**, 87–184.
CHANG, S. L., KING, H. E. JR, HUANG, M. T. & GAO, Y. (1991). *Phys. Rev. Lett.* **67**, 3113–3116.
CHAPMAN, L. D., YODER, D. R. & COLELLA, R. (1981). *Phys. Rev. Lett.* **46**, 1578–1581.
COLELLA, R. (1974). *Acta Cryst.* A**30**, 413–423.
COLELLA, R. (1982). *Z. Naturforsch. Teil A*, **37**, 437–447.
CORNIER-QUIQUANDON, M., QUIVY, A., LEFÈBVRE, S., ELKAIM, E., HEGER, G., KATZ, A. & GRATIAS, D. (1991). *Phys.*
ELSER, V. (1986). *Acta Cryst.* A**42**, 36–43, Appendix, § 2, equations (21) and (23).
ELSER, V. (1991). Private communication.
HÜMMER, K., SCHWEGLE, W. & WECKERT, E. (1991). *Acta Cryst.* A**47**, 60–62.
JANOT, C., PANNETIER, J., DE BOISSIEU, M. & DUBOIS, J. M. (1987). *Europhys. Lett.* **3**, 995–1000.
RZEPSKY, J. D., QUIVY, A., CALVAYRAC, Y., CORNIER-QUIQUANDON, M. & GRATIAS, D. (1989). *Philos. Mag.* B**60**, 855–869.
SHEN, Q. (1986). *Acta Cryst.* A**42**, 525–533.
SHEN, Q. & COLELLA, R. (1987). *Nature (London)*, **329**, 232–233.
TISCHLER, J. Z., SHEN, Q. & COLELLA, R. (1985). *Acta Cryst.* A**41**, 451–453.

Acta Cryst. (1993). A**49**, 605–613

Effects of a General X-ray Polarization in Multiple-Beam Bragg Diffraction

BY QUN SHEN

Cornell High-Energy Synchrotron Source (CHESS) and Department of Applied Engineering Physics, Cornell University, Ithaca, New York 14853, *USA*

(*Received* 12 *October* 1992; *accepted* 22 *December* 1992)

Abstract

The formalism of the *N*-beam dynamical theory of X-ray diffraction is extended to include all possible incident and diffracted polarizations. With this new formalism it is shown that the intensity of a simultaneously excited Bragg reflection can be described through a polarization density matrix that involves the Stokes–Poincaré parameters. In particular, the multibeam diffracted intensity is sensitive to the circularly polarized component in the incident beam and the structure-factor phases of the diffracting crystal. Experimental results on the GaAs 442 and Ge 333 reflections confirm the theoretical calculations. This kind of measurement can provide useful acentric phase information and can also be used for circular X-ray polarimetry. Another feature of *N*-beam diffraction is its ability to turn a linear polarization into an elliptical polarization, which means it can be used as an X-ray phase plate.

Introduction

X-ray polarization plays an important role in every scattering and diffraction experiment. In crystallography, one needs to use the polarization-factor correction in order to obtain structure factors from diffracted intensities (Warren, 1969). In X-ray physics and